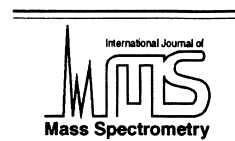




ELSEVIER

International Journal of Mass Spectrometry 208 (2001) 245–247



## Subject index

### Ab initio calculations

Ab initio calculations on the isomerization of  $C_4H_6$  radical cations, 119

### Absolute cross sections

Experimental investigation of the formation of N atoms in  $N^+-Ne$ , Kr, and Xe collisions, 81

### Abundance sensitivity

Quadrupole mass filter operation with auxiliary quadrupolar excitation: theory and experiment, 17

### Actinides

Ultratrace and isotopic analysis of long-lived radionuclides by double-focusing sector field inductively coupled plasma mass spectrometry using direct liquid sample introduction, 193

### Ammonia phosphorus oxide

Characterization of ammonia phosphorus oxide  $H_3NPO^+$  ions and their neutral counterparts by mass spectrometry and computational chemistry, 59

### Angular distributions

Experimental investigation of the formation of N atoms in  $N^+-Ne$ , Kr, and Xe collisions, 81

### Atomic weight

Absolute isotopic composition and atomic weight of zinc, 113

### Blister agent

Static secondary ionization mass spectrometry and mass spectrometry/mass spectrometry ( $MS^2$ ) characterization of the chemical warfare agent HD on soil particle surfaces, 135

### Carbon

Structures and energies of  $C_nS^+$  ( $1 \leq n \leq 16$ ) and  $C_nS^-$  ( $9 \leq n \leq 16$ ) clusters, 7

### Chemical agent

Static secondary ionization mass spectrometry and mass spectrometry/mass spectrometry ( $MS^2$ ) characterization of the chemical warfare agent HD on soil particle surfaces, 135

### CHF<sub>3</sub>

Electron impact ionization of CHF<sub>3</sub>, 159

### C<sub>4</sub>H<sub>6</sub> radical cations

Ab initio calculations on the isomerization of  $C_4H_6$  radical cations, 119

### Clusters

Sputtering of a Au surface covered with large spherical clusters, 29

Structures and energies of  $C_nS^+$  ( $1 \leq n \leq 16$ ) and  $C_nS^-$  ( $9 \leq n \leq 16$ ) clusters, 7

### CN radical

Product channeling in the reactions of  $CS^+(X^2\Sigma^+)$  with simple carboxylic acids and esters, 99

### Collisional activation

Characterization of ammonia phosphorus oxide  $H_3NPO^+$  ions and their neutral counterparts by mass spectrometry and computational chemistry, 59

### Computational chemistry

Characterization of ammonia phosphorus oxide  $H_3NPO^+$  ions and their neutral counterparts by mass spectrometry and computational chemistry, 59

### Cross sections

Electron impact ionization of the  $TiCl_x$  ( $x = 1 - 3$ ) free radicals, 1

### CS<sup>+</sup> ion

Product channeling in the reactions of  $CS^+(X^2\Sigma^+)$  with simple carboxylic acids and esters, 99

### Desorption

Sputtering of a Au surface covered

with large spherical clusters, 29

### DFT

Structures and energies of  $C_nS^+$  ( $1 \leq n \leq 16$ ) and  $C_nS^-$  ( $9 \leq n \leq 16$ ) clusters, 7

### Direct injection high efficiency nebulizer

Ultratrace and isotopic analysis of long-lived radionuclides by double-focusing sector field inductively coupled plasma mass spectrometry using direct liquid sample introduction, 193

### Dissociative

Comparisons of electron impact ionization and ion chemistries of  $CF_3Br$  and  $CF_3I$ , 127

### Distilled mustard

Static secondary ionization mass spectrometry and mass spectrometry/mass spectrometry ( $MS^2$ ) characterization of the chemical warfare agent HD on soil particle surfaces, 135

### Double-focusing sector field inductively coupled plasma mass spectrometry

Ultratrace and isotopic analysis of long-lived radionuclides by double-focusing sector field inductively coupled plasma mass spectrometry using direct liquid sample introduction, 193

### Drift velocity

Pulsed injection of ions into the CRESU experiment, 73

### Electron impact ionization

Electron impact ionization of CHF<sub>3</sub>, 159

Electron impact ionization of the  $TiCl_x$  ( $x = 1 - 3$ ) free radicals, 1

### Electron transfer

Experimental investigation of the formation of N atoms in  $N^+-Ne$ , Kr, and Xe collisions, 81

- Electrospray  
 Ion discrimination during ion accumulation in a quadrupole interface external to a Fourier transform ion cyclotron resonance mass spectrometer, 205
- Fractionation  
 High-precision measurement of magnesium isotopes by multiple-collector inductively coupled plasma mass spectrometry, 89
- Fragmentation  
 Ab initio calculations on the isomerization of  $C_4H_6$  radical cations, 119
- FTICR-MS (Fourier transform ion cyclotron resonance mass spectrometry)  
 Ion discrimination during ion accumulation in a quadrupole interface external to a Fourier transform ion cyclotron resonance mass spectrometer, 205
- High order resonance  
 Quadrupole mass filter operation with auxiliary quadrupolar excitation: theory and experiment, 17
- Ion chemistry  
 Comparisons of electron impact ionization and ion chemistries of  $CF_3Br$  and  $CF_3I$ , 127
- Ion discrimination  
 Ion discrimination during ion accumulation in a quadrupole interface external to a Fourier transform ion cyclotron resonance mass spectrometer, 205
- Ion emission mechanisms  
 Ag ion formation mechanisms in molten glass ion emitters, 37
- Ionization  
 Comparisons of electron impact ionization and ion chemistries of  $CF_3Br$  and  $CF_3I$ , 127
- Ion mobility spectrometry  
 Characterization of the ion-sampling pinhole interface for an ion mobility spectrometer/mass spectrometer system, 169  
 Gas-phase ion mobility studies of constitutional isomeric hydrocarbons using different ionization techniques, 67
- Ion/molecule reactions  
 Product channeling in the reactions of  $CS^+(X^2\Sigma^+)$  with simple carboxylic acids and esters, 99  
 Pulsed injection of ions into the CRESU experiment, 73
- Ion-sampling  
 Characterization of the ion-sampling pinhole interface for an ion mobility spectrometer/mass spectrometer system, 169
- Ion stability  
 Ion discrimination during ion accumulation in a quadrupole interface external to a Fourier transform ion cyclotron resonance mass spectrometer, 205
- Isomeric alkyl benzenes  
 Gas-phase ion mobility studies of constitutional isomeric hydrocarbons using different ionization techniques, 67
- Isomerization  
 Ab initio calculations on the isomerization of  $C_4H_6$  radical cations, 119
- Isotope ratio analysis  
 Ultratrace and isotopic analysis of long-lived radionuclides by double-focusing sector field inductively coupled plasma mass spectrometry using direct liquid sample introduction, 193
- Isotope ratios  
 Ag ion formation mechanisms in molten glass ion emitters, 37
- Isotopic abundance  
 Absolute isotopic composition and atomic weight of zinc, 113
- Isotopic ratio measurements  
 Isotopic ratio measurements by time-of-flight secondary ion mass spectrometry, 227
- Low temperature  
 Pulsed injection of ions into the CRESU experiment, 73
- Mass-dependent  
 High-precision measurement of magnesium isotopes by multiple-collector inductively coupled plasma mass spectrometry, 89
- Mass spectrometry  
 Absolute isotopic composition and atomic weight of zinc, 113
- Mg  
 High-precision measurement of magnesium isotopes by multiple-collector inductively coupled plasma mass spectrometry, 89
- Molecular-dynamics simulation  
 Sputtering of a Au surface covered with large spherical clusters, 29
- Molten glass  
 Ag ion formation mechanisms in molten glass ion emitters, 37
- $N^0$   
 Experimental investigation of the formation of N atoms in  $N^+-Ne, Kr,$  and  $Xe$  collisions, 81
- $N^+$   
 Experimental investigation of the formation of N atoms in  $N^+-Ne, Kr,$  and  $Xe$  collisions, 81
- Neutralization reionization  
 Characterization of ammonia phosphorus oxide  $H_3NPO^+$  ions and their neutral counterparts by mass spectrometry and computational chemistry, 59
- Photoelectron-photoion coincidence data  
 Behavior of excited  $C_3H_6O^+$  cations: a He-I $\alpha$  photoelectron-photoion coincidence study of propanal, 147
- Plasma deposition  
 Electron impact ionization of the  $TiCl_x$  ( $x = 1 - 3$ ) free radicals, 1
- Product distributions  
 Product channeling in the reactions of  $CS^+(X^2\Sigma^+)$  with simple carboxylic acids and esters, 99
- Propanal  
 Behavior of excited  $C_3H_6O^+$  cations: a He-I $\alpha$  photoelectron-photoion coincidence study of propanal, 147
- Propanal cation  
 Behavior of excited  $C_3H_6O^+$  cations: a He-I $\alpha$  photoelectron-photoion coincidence study of propanal, 147
- Pseudohalogen  
 Product channeling in the reactions of  $CS^+(X^2\Sigma^+)$  with simple carboxylic acids and esters, 99

- Pulsed ion source  
Pulsed injection of ions into the CRESU experiment, 73
- Quadrupole mass filter  
Quadrupole mass filter operation with auxiliary quadrupolar excitation: theory and experiment, 17
- Quasi-equilibrium theory calculations  
Behavior of excited  $C_3H_6O^+$  cations: a He-I $\alpha$  photoelectron-photoion coincidence study of propanal, 147
- Radioactive waste  
Ultratrace and isotopic analysis of long-lived radionuclides by double-focusing sector field inductively coupled plasma mass spectrometry using direct liquid sample introduction, 193
- Rate coefficients  
Product channeling in the reactions of  $CS^+(X^2\Sigma^+)$  with simple carboxylic acids and esters, 99
- Resolution  
Quadrupole mass filter operation with auxiliary quadrupolar excitation: theory and experiment, 17
- Resonance excitation  
Quadrupole mass filter operation with auxiliary quadrupolar excitation: theory and experiment, 17
- Secondary ion mass spectrometry  
Static secondary ionization mass spectrometry and mass spectrometry/mass spectrometry ( $MS^2$ ) characterization of the chemical warfare agent HD on soil particle surfaces, 135
- Selective external ion accumulation  
Ion discrimination during ion accumulation in a quadrupole interface external to a Fourier transform ion cyclotron resonance mass spectrometer, 205
- Silica gel  
Ag ion formation mechanisms in molten glass ion emitters, 37
- SIMS  
Isotopic ratio measurements by time-of-flight secondary ion mass spectrometry, 227
- Sputtering  
Sputtering of a Au surface covered with large spherical clusters, 29
- Stability "islands"  
Quadrupole mass filter operation with auxiliary quadrupolar excitation: theory and experiment, 17
- Standard, SRM980  
High-precision measurement of magnesium isotopes by multiple-collector inductively coupled plasma mass spectrometry, 89
- Structure  
Structures and energies of  $C_nS^+$  ( $1 \leq n \leq 16$ ) and  $C_nS^-$  ( $9 \leq n \leq 16$ ) clusters, 7
- Sulfur  
Structures and energies of  $C_nS^+$  ( $1 \leq n \leq 16$ ) and  $C_nS^-$  ( $9 \leq n \leq 16$ ) clusters, 7
- Surface analysis  
Static secondary ionization mass spectrometry and mass spectrometry/mass spectrometry ( $MS^2$ ) characterization of the chemical warfare agent HD on soil particle surfaces, 135
- Surface roughness  
Sputtering of a Au surface covered with large spherical clusters, 29
- Thermal ion emission  
Ag ion formation mechanisms in molten glass ion emitters, 37
- Titanium tetrachloride  
Electron impact ionization of the  $TiCl_x$  ( $x = 1 - 3$ ) free radicals, 1
- ToF-SIMS  
Isotopic ratio measurements by time-of-flight secondary ion mass spectrometry, 227
- Tunneling  
Ab initio calculations on the isomerization of  $C_4H_6$  radical cations, 119
- Uniform supersonic jet  
Pulsed injection of ions into the CRESU experiment, 73
- Vapor viscosity  
Product channeling in the reactions of  $CS^+(X^2\Sigma^+)$  with simple carboxylic acids and esters, 99
- Zinc  
Absolute isotopic composition and atomic weight of zinc, 113